Letters in Applied NanoBioScience
Open-Access Journal (ISSN: 2284-6808)

Article
Volume 12, Issue 2, 2023, 39
https://doi.org/10.33263/LIANBS122.039

Solvent Effect and Pigment Reaction in Black Cherry

Fatemeh Mollaamin [1,*]

[1] Department of Biomedical Engineering, Faculty of Engineering and Architecture, Kastamonu University, Kastamonu, Turkey
* Correspondence: smollaamin@gmail.com (F.M.);

Scopus Author ID 35848813100
Received: 29.11.2021; Accepted: 28.12.2022; Published: 16.03.2022

Abstract: In this investigation, theoretical infrared spectroscopy has been applied to distinguish the functional group of the compounds to calculate their physical and chemical properties for approving frequency and intensity of absorbance in six water-soluble anthocyanins, including Cyanidin (Cya), Pelargonidin (Pel), Peonidin (Peo), Delphinidin (Del), Malvidin (Mal) and Petunidin (Pet) in vacuum and water media with a variety of pH. As Anthocyanins are more stable at low pH acidic conditions meanwhile, the higher amount of pH among anthocyanins will indicate a colorless medium. In this work, it has been illustrated the electronic structure of anthocyanin pigments that changes due to the solvent dielectric effect of polar H_2O molecules. Most anthocyanins in nature have been derived from six anthocyanidin aglycones of flavylium chain with various glycosylations and acylations consisting of Cyanidin, Pelargonidin, Peonidin, Delphinidin, Malvidin, and Petunidin. In this work, it has been studied the information available concerning the electronic structure thermodynamic properties of these anthocyanin pigments in vacuum and water media at 300K toward approving their stability and color. Different water-soluble anthocyanins absorb the light and produce red, blue, and purple colors in vegetables and fruits.

Keywords: solvent effect; anthocyanin pigments; water; thermodynamic properties.

1. Introduction

The cherry tree belongs to the Rosaceae family, including peaches, apricots, and plums. This tree is native to the Caspian region, the Black Sea, and northeastern Anatolia and has spread across the world [1,2]. The two most consumed species are wild or sweet cherries and sour cherries or sour cherries.

The main characteristics linked to the quality of the cherry are its color, sweetness, acidity, and firmness. The pigments responsible for the color of the cherry are anthocyanins. Their content varies depending on the cultivar, which gives them colors ranging from yellow to dark red. The cherry's sweetness is believed to be due to its fructose and glucose content, followed by arabinose and sorbitol. Its acidity could be explained by the presence of organic acids, mainly malic acid, followed by ascorbic, tartaric, and shikimic acid. In sour cherries or sour cherries, fructose is the predominant sugar, glucose, sorbitol, and sucrose. The polysaccharide composition of the cherry cell wall could have an important influence on the firmness of the fruit [3-5].

Thirty-one volatile compounds have been isolated from seven Spanish cultivars, including acids, alcohols, and aldehydes. The six compounds responsible for the aroma of the

cherry would be benzaldehyde, benzyl alcohol, eugenol, nonanal, trans-2-hexenal, and isoamyl butyrate [5, 6].

Cherries contain carotenoids, more specifically β-carotene and lutein and, to a lesser extent, zeaxanthin. Cherries (sweet or sour) contain an interesting amount of polyphenols (Phenol Explorer). Among them, anthocyanins have multiple properties: antioxidant and anti-inflammatory properties that promote recovery after exercise and lower blood pressure; they could also decrease the blood concentrations of biomarkers linked to the degradation of skeletal muscles and reduce the risks of cardio-metabolic diseases (hypertension and dyslipidemia); they could reduce the risk of several degenerative diseases, such as cancer and heart disease. The consumption of cherries is even associated with a reduction in arthritis and pain associated with gout with methanol; they would have anticancer powers, particularly on prostate cancer, by stimulating apoptosis of cancer cells [6, 7].

Anthocyanins are mostly 3-glucosides of anthocyanidins. Anthocyanins are subdivided into sugar-free anthocyanidins aglycones and anthocyanins glycosides. The difference in chemical structure that occurs in response to changes in pH is why anthocyanins are often used as pH indicators, as they change from red in acids to blue in bases through a process called halochromism [8,9].

It is believed that anthocyanins are subject to physicochemical degradation *in vivo* and *in vitro*. The structure, pH, temperature, light, oxygen, metal ions, intramolecular association, and intermolecular association with other compounds (copigments, sugars, proteins, degradation products, etc.) are generally known to affect the color and stability of anthocyanins.The B-ring hydroxylation state and pH have been shown to be involved in the degradation of anthocyanins to their phenolic acid and aldehyde constituents. Indeed, large portions of ingested anthocyanins are liable to degrade into phenolic acids and aldehyde *in vivo*, after consumption. This characteristic confuses the scientific isolation of the specific mechanisms of anthocyanin *in vivo* [10].

Anthocyanins are secondary metabolites of plants generally located in vacuoles. Their bright color attracts insects and birds, which play a major role in pollinating flowers and dispersing seeds. The main physiological roles attributed to them in the plant are, among others, the absorption of harmful radiations for chlorophyll b, the transport of monosaccharides, the regulation of osmotic pressure during periods of drought and cold, or the regulation of the antioxidative response of plants subjected to stress factors [10,11].

They are particularly studied for their notorious stability problem, the positive effect of their consumption on health, and their potential as a natural food coloring. These are the areas that will be addressed in the following literature review to review the use of fruits and vegetables rich in anthocyanins as sources of food coloring.

Anthocyanidins, polyhydroxy derivatives of the flavylium ion (2-phenylbenzopyrylium), are differentiated by the number and location of hydroxyl and methoxyl groups. Although 31 anthocyanidins have been identified, 90% of anthocyanins are derived from 6 anthocyanidins of Cyanidin, Delphinidin, Malvidin, Pelargonidin, Peonidin, and Petunidin. Many combinations are thus possible, and nearly 600 compounds have been identified. The color of anthocyanins is the most notable characteristic is the change of color which accompanies the variations of pH of their medium. As the pH increases, structural changes resulting from hydration and proton transfer reactions cause changes in structure and color. As a result, several resonant shapes and structures can coexist in a complex medium for the same type of anthocyanin. This is explained by conjugating all the π bonds of the A and C

rings. These color changes lead to the limitation of their use as a red food coloring to foodstuffs having a pH lower than 5; in addition, they are particularly sensitive to the treatments that these foodstuffs could subsequently undergo [11,12].

Under certain pH and temperature conditions, anthocyanins degrade in the presence of oxygen, metal ions, enzymes, and light. This degradation is accompanied by an increase in the concentration of compounds formed by the condensation between the degradation products of anthocyanins and other polyphenols present in the medium. This results in the formation of polymers that become larger and tend to precipitate over time. The medium's acidity affects the color and the reactivity of anthocyanins. The increase in pH causes the C-ring to open by nucleophilic attack giving the hemiacetal form whose reactivity is greater than that of the flavylium ion. In a strongly acidic medium (pH <2), anthocyanins show good stability with respect to temperature and oxygen. On the other hand, their degradation accelerates when the pH increases under the same temperature and aeration conditions. In addition to color, differences in structure result in different reactivity in anthocyanins, resulting in greater stability generally observed in more complex anthocyanins. Substitutions affect the stability of anthocyanins mainly through a phenomenon called copigmentation. It occurs when the substituents of an acylated anthocyanin or molecules present in the medium help produce a protective hydrophobic environment around the flavylium nucleus. This effect becomes significant only when there is an overabundance of protective molecules compared to anthocyanin molecules [12].

2. Materials and Methods

The theoretical methods to obtain models that can predict and understand molecular structures, properties, and interactions of anthocyanins are used in this study. This makes it possible to provide information that is not available from experience and therefore plays a role complementary to experimental chemistry. Thus, molecular modeling can make it anthocyanins possible to get a precise idea of the structure of the transition state for a given reaction. Anthocyanins are heat-labile and degrade at a rate that increases considerably with temperature. They are, however, relatively stable for temperatures below 70°C. Thermo degradation at 95°C and pH = 1 begins after 4 h with deglycosylation followed by cleavage, leading to the release of anthocyanidin's A and B rings. Storage of anthocyanins at low temperatures allows very good preservation of their color. The presence of oxygen causes the degradation of anthocyanins by a mechanism that may be chemical oxidation or an enzymatic reaction in the presence of polyphenol oxidase. PPO is an endogenous enzyme responsible for the browning phenomenon of fruits. It oxidizes polyphenols to quinones, which combine with anthocyanins to form brown compounds according to the mechanism shown. Heat treatment at 50 ° C significantly reduces the effect of this enzyme [13-15]. In this investigation, the DFT calculations were also carried out using the GAUSSIAN09 with the functional B3LYP on 6 anthocyanins' families [16].

The city of Oshnavieh in the province of West Azerbaijan with 300 hectares of cherry orchards is known as the cherry capital of the country. Cherry harvest begins in the first days of July and continues until the second half of this month. More than 1,500 tons of cherries are expected to be harvested this year. More than 90% of this product enters the domestic and foreign markets as fresh food. In the harvest season of this product, more than 5,000 people are directly and indirectly employed (Scheme 1a). Classified among flavonoids, anthocyanins are characterized by the C6-C3-C6 backbone (Scheme 1b). These are glucosides formed from the

combination of an aglycone called anthocyanidin and a sugar substituted in position 3. These sugars, which are of the mono-, di- or tri-saccharide type can be acylated by aliphatic acids or aromatic [17-20].

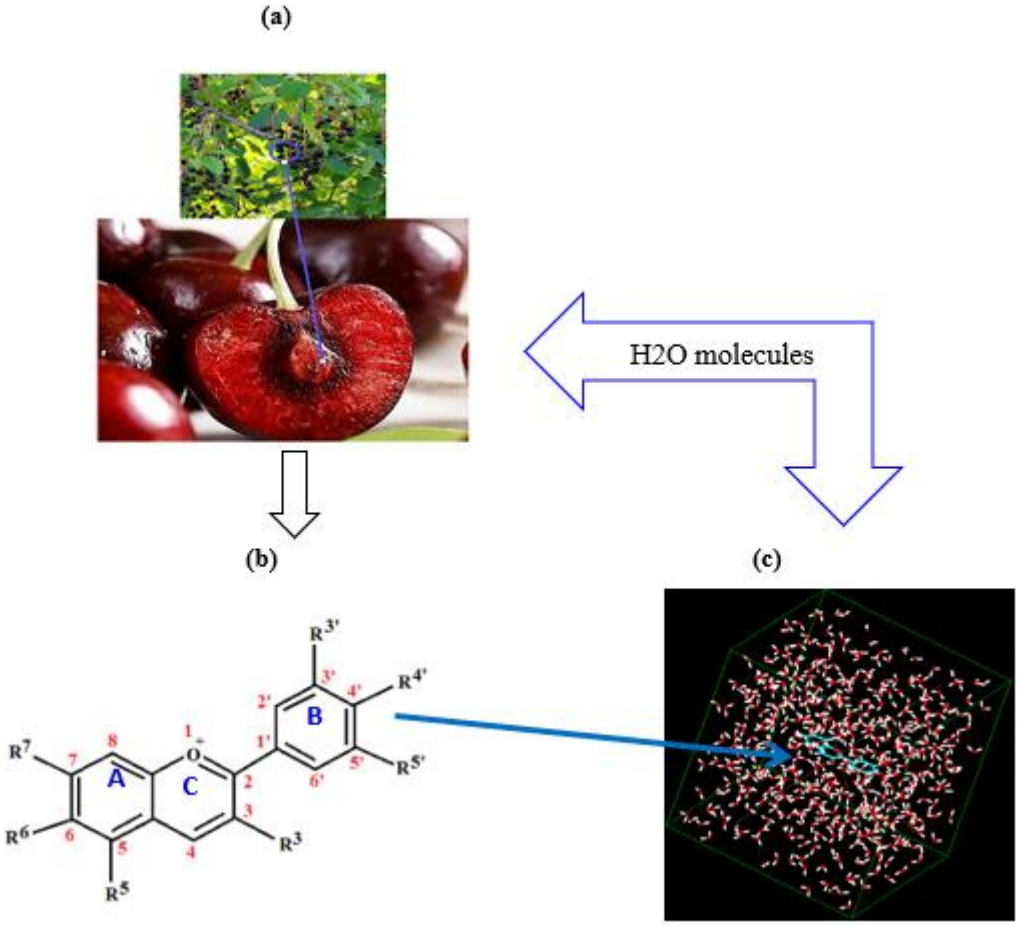

Scheme1. (a) Cherry of Oshnavieh garden in Iran; **(b)** Schematic of anthocyanin molecule (solute); **(c)** Solvation optimized model of anthocyanins' family in water molecules (solvent) at 300K.

Most chemical reactions, and almost all biochemical reactions, occur in solution. The effects of the solvent on the chemical reactivity of the species are not negligible. Therefore, it is necessary to do the optimized geometry, charge electron transfer, and thermodynamic properties of 6 anthocyanidins of Cyanidin, Delphinidin, Malvidin, Pelargonidin, Peonidin, and Petunidin in the water environment. The optimized geometry, charge electron transfer, and thermodynamic properties of 6 anthocyanidins of Cyanidin, Delphinidin, Malvidin, Pelargonidin, Peonidin, and Petunidin in vacuum and water media at 300K have been measured and compared with each other by different concentrations of H^+ in a simulated solvent model of H_2O molecules (Scheme 1a-c).

The method used to implement such a model is called SCRF (for self-consistent reaction field). The expression of the electronic wave function and that of the probability density solute electronics change when going into solution. This helps ensure self-consistency between the solute's charge distribution and the solvent's reaction field (the field generated by the solvent polarized around the solute). The Schrödinger equation is solved for an equal total Hamiltonian :

$$\hat{H}_A^{(0)} + \hat{V}_{int} \qquad (1)$$

Several models are used in SCRF. They differ according to two main criteria: part, depending on the shape and size of the cavity containing the solute; and secondly, in the way

$\hat{V}_{int}$ is calculated. Not all models will be included in this section; only those necessary to understand this work are presented [21-26].

The Onsager model is the simplest. The cavity containing the solvent is considered to be a sphere. The interaction potential, $\hat{V}_{int}$, is calculated by describing the charge distribution of the solute by an electric dipole located in the center of the cavity. An improvement of the Onsager model considers the ellipsoidal shaped cavity and models the charge distribution of solute by the multipolar expression [27-30].

The PCM model (polarizable continuum model) describes more precisely the solvent effects than the Onsager model. It more realistically models the shape of the cavity. In the PCM model, each atomic nucleus of solute is surrounded by a sphere whose radius is equal to 1.2 times. The cavity is the region whose volume is delimited by the entanglement of these spheres. The value of $\hat{V}_{int}$ is determined by means of an analytical method. Electrostatic potential produced by the polarized dielectric medium is equal to the potential produced by an apparent load. It is a load continuously distributed on the surface of the cavity and characterized by a surface charge density that varies from point to point on the surface. According to Onsager's theory, a dielectric cannot spontaneously polarize under the sole influence of the classical dipole-dipole interaction. Onsager method only leads to a lowering of the Curie point, the importance of which we can moreover assess. This conclusion is important to the subject of Ferroelectricity, which is often attributed to the dipolar interaction. In addition, it could explain that the 4π/ 3 catastrophe did not manifest itself in certain crystals where it was expected to be observed. For this reason, Onsager has built a theory where correlations play an essential role and moreover overestimated. The resulting equation [31-36]:

$$\frac{(\varepsilon-1)(2\varepsilon+1)}{\varepsilon} = 4\pi N \frac{\mu^2}{kT} \qquad (2)$$

However, the small temperature admits a positive solution. We thought we could deduce from this that the Onsager method necessarily ruled out any possibility of spontaneous polarization under the influence of the classical interaction between dipoles.

The mutual interaction between classical, electric, or magnetic is likely to cause the polarization of a crystal. An affirmative answer is indeed provided by Debye's theory of dielectrics, a theory formally identical to Weiss theory of ferromagnetism, but in which the molecular field is given by the Lorentz-Lorenz formula [37- 41]:

$$\vec{F} = f\vec{P} \qquad (3)$$

$$\vec{F} = \vec{E} + \frac{4\pi}{3}\vec{P} \qquad (4)$$

The Lorentz factor / having the value 4π/3 in the case of networks cubic, but such a theory neglects the influence of the structure crystalline, except for the evaluation of statistical correlations between the orientations of the neighboring dipoles: only the mean value of the polarization is involved in the calculation of the total energy of the crystal

It follows, first of all, from this approximation that the minimum energy state would correspond to the maximum polarization state, where all the dipoles are parallel. This conclusion is certainly incorrect in the case of the simple cubic lattice, where we have found zero polarization states whose energy is lower than that of the maximum polarization state. However, it does seem that this circumstance no longer occurs in networks where the number of immediate neighbors is higher, for example, in cubic networks with body-centered and faces centered [42-47].

Things are no longer so simple if we admit a priori that the dielectric is spontaneously polarized. If the polarization is not more proportional to the field, we would have to solve a

non-linear problem very difficult. However, if the temperature is low enough, we can assume that the dielectric is very strongly polarized so that the polarization is, as a first approximation, a linear function of $\vec{E}$ [47, 48]:

$$P(T) = P_0\,(T) + \left(\frac{\partial P(T)}{\partial E}\right)_{E=0} . E \qquad (5)$$

We immediately see that Onsager's reasoning remains because it requires only the linearity of the relation uniting *P* h *E*; simple proportionality is by no means necessary [48,49]. Thus, we will have to consider a fictitious dielectric whose susceptibility and dielectric constant are:

$$x = \frac{\partial P}{\partial E} \qquad (6)$$

$$\varepsilon = 1 + 4\pi x \qquad (7)$$

For obtaining the potential V which corresponds to the cavity field, it suffices to solve the Laplace equation $\Delta V = 0$ with the condition: $V(r_0 - 0, \theta) = V(r_0 + 0, \theta)$ (8)

3. Results and Discussion

Anthocyanins are naturally present in many foods eaten regularly, especially red fruits. The moderately consumed amounts vary depending on the country and eating habits. They are studied for the positive effects of their consumption on health. These effects are generally attributed to their antioxidant power, which would allow them to protect tissues against damage caused by free radicals. They can thus have a preventive effect by reducing the damage that the accumulation of free radicals could cause. Their consumption is associated with improving visual acuity; they are recognized as having anticarcinogenic and anti-inflammatory properties and the ability to reduce the risks of being affected by cardiovascular diseases [50].

In this investigation, the pigments of Cyanidin (Cya), Delphinidin (Del), Malvidin(Mal), Pelargonidin (Pel), Peonidin (Peo), and Petunidin(Pet) have been calculated using theoretical methods to evaluate the dielectric solvent effect on the stability of these anthocyanins in vacuum and water media at 300 K (Scheme 1a-c).

In this investigation, we showed that the central quantity of a system in thermodynamic equilibrium is its canonical partition function which function belongs to a single harmonic oscillator can be calculated analytically. So, we generalize any harmonic system for the energies of the stationary states. This greatly facilitates the calculation of thermodynamic functions. You just need to know the density of states. We have calculated the internal energy and vibrational calculation of the system with its eigenvector for finding thermodynamic parameters and physical properties of anthocyanins including ΔG,ΔH, ΔS lnK, Electronic Energy, and Core-Core Interaction have been calculated by Gaussian09 in vacuum and water media at 300K [16] (Table1 and Figure1a,b). These results show how the density of states plays a central role in calculating macroscopic thermodynamic quantities.

Table 1. Thermodynamic properties of anthocyanins of Cya, Del, Mal, Pel, Peo, Pet in vacuum and water media at 300K.

Pigment	ΔG (kcal/mol)	ΔH (kcal/mol)	ΔS ×10^{-2} (kcal/K.mol)	$E_{electronic}$ (kcal/mol)	$E_{core-core}$ (kcal/mol)	lnK ×10^{-5}
Cya (vacuum)	-9.20×10^3	-9.15×10^1	3.07	-5.50×10^5	4.8×10^5	1.54
Cya (water)	-2.85×10^5	-1.54×10^3	9.44	-2.80×10^6	2.51×10^6	2.85
Del(vacuum)	-9.94×10^4	-1.34×10^2	3.31	-6.02×10^5	5.02×10^5	1.66
Del(water)	-2.92×10^5	-1.57×10^3	9.69	-2.89×10^6	2.60×10^6	4.90

Pigment	ΔG (kcal/mol)	ΔH (kcal/mol)	ΔS ×10^{-2} (kcal/K.mol)	$E_{electronic}$ (kcal/mol)	$E_{core-core}$ (kcal/mol)	lnK ×10^{-5}
Mal(vacuum)	-1.06×10^5	-1.05×10^2	3.55	-7.05×10^5	5.98×10^5	1.78
Mal(water)	-2.11×10^5	-9.07×10^2	7.00	-1.86×10^6	1.65×10^6	3.54
Pel(vacuum)	-8.46×10^4	-5.18×10^1	2.82	-5.01×10^5	4.16×10^5	1.42
Pel(water)	-2.45×10^5	-1.26×10^3	8.14	-2.25×10^6	2.01×10^6	1.37
Peo(vacuum)	-9.56×10^4	-7.74×10^1	3.18	-5.98×10^5	5.03×10^5	1.60
Peo(water)	-2.72×10^5	-1.42×10^3	9.03	-2.61×10^6	2.33×10^6	4.56
Pet(vacuum)	-1.03×10^5	-1.20×10^2	3.43	-6.53×10^5	5.50×10^5	1.72
Pet(water)	-2.80×10^5	-1.47×10^3	9.28	-2.75×10^6	2.47×10^6	4.69

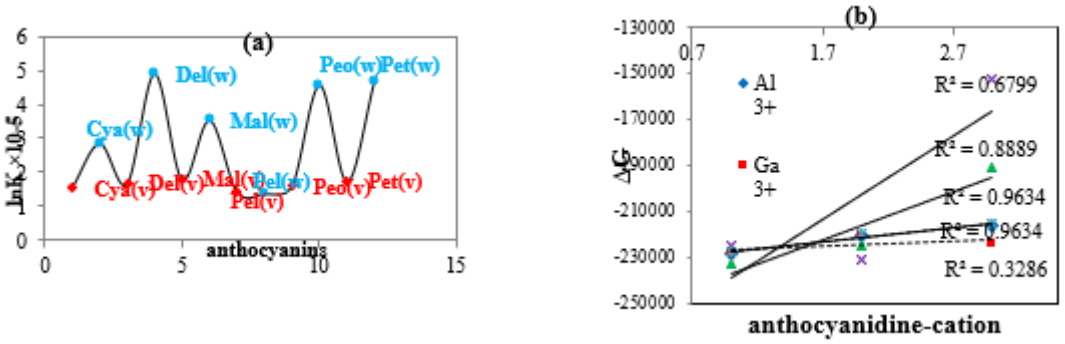

Figure1. (a) The calculated equilibrium constant (K) of anthocyanin pigments of Cya, Del, Mal, Pel, Peo, Pet in vacuum and water at 300K. **(b)** Changes of Gibbs free energy (Δ*G*, kcal/mol) of [ACN- Mg^{2+}/Al^{3+}/Ga^{3+}/ Sn^{2+}/Cr^{3+}/Fe^{3+}] chelation water at 330K.

It is interesting to extract as much information as possible without resorting to explicit calculations. Such information is extracted from the symmetry properties of the system: symmetry establishes relations between the constants of force and thus reduces the degrees of freedom of the dynamic matrix. The forces between two sets of atoms that are images of each other under an operation of symmetry are identical.

The difference between these subclasses is revealed of double bonds and carbonyl groups in the C ring in vacuum and water media that approves the stability and color of anthocyanins pigments in a weak acidic condition (Figure1a,b). The slope of the straight differs from compound to compound. To explain this behavior, remember that the free energy of a molecule is given by the difference between its enthalpy and the product of its entropy by temperature according to:

$$G = H - TS \qquad (9)$$

Let us study the behavior of ΔG when the temperature varies. The value of ΔH depends on the temperature. Indeed :

$$H = E_{tot} + k_b T \qquad (10)$$

and E_{tot} depends on the temperature through its contributions translational (E_{trans}) rotational (E_{rot}), and vibrational (E_{vib}), which are functions of the temperature. The value of ΔS depends on the temperature. Indeed:

$$S = S_{trans} + S_{elec} + S_{rot} + S_{vib} \qquad (11)$$

where S_{trans}, S_{elec}, S_{rot}, S_{vib} depend respectively on translational contributions, electronic, rotational, and vibrational to the function of total partition of the system, q_{tot}. The latter is also a function of temperature (and pressure). Note S_{vib} also depends directly from the temperature through the term T ($\frac{\partial lnq}{\partial T}$) [50-52]. It appears that for the domain of temperature studied and for the molecules considered, the values of H and S of a molecule vary slightly when the temperature increases (Figure1a,b).

Absorbance (A), the proportion of light absorbed by a solution at a certain wavelength, was calculated for six anthocyanins pigments of Cya, Del, Mal, Pel, Peo, Pet in a water medium (Table 2). The color of a solution is related to its absorbance, a quantity that can be measured using a spectrophotometer. We measure the absorbance A of a solution at different wavelengths. Thus, the absorption spectrum is obtained:

$$A = f(\lambda) \quad (12)$$

The absorbance of a solution is proportional to its concentration:

$$A = \varepsilon x l x C \quad (13)$$

Table 2. Calculated absorbance (A), frequency, and dipole of anthocyanin pigments of Cya, Del, Mal, Pel, Peo, and Pet in different pH.

Cya			
pH	**A**	**Frequency (1/cm)**	**Dipole (Debyes)**
0.84	1.96	3518.59	5.47
0.95	1.95	3518.59	5.46
1.11	0.25	3602.86	4.15
1.28	0.79	3617.99	2.40
1.48	1.66	3644.25	8.68
1.60	1.50	3657.02	4.44
Del			
pH	**A**	**Frequency (1/cm)**	**dipole (Debyes)**
0.84	1.71	3647.81	8.89
0.95	1.70	3647.81	8.88
1.11	1.66	3646.86	9.06
1.28	1.68	3647.42	9.07
1.48	1.59	3650.29	8.49
1.60	1.62	3682.85	11.93
Mal			
pH	**A**	**Frequency (1/cm)**	**Dipole (Debyes)**
0.84	2.10	3521.74	6.70
0.95	1.49	3521.74	6.69
1.11	0.66	3613.85	9.92
1.28	0.66	3613.87	9.87
1.48	0.03	3662.21	5.52
Pel			
pH	**A**	**Frequency (1/cm)**	**dipole (Debyes)**
0.84	2.09	3522.11	4.36
0.95	2.08	3522.11	4.35
1.11	2.07	3522.11	4.36
1.28	1.50	3649.06	4.82
1.48	1.56	3656.27	7.94
1.60	1.71	3677.06	3.97
Peo			
pH	**A**	**Frequency (1/cm)**	**dipole (Debyes)**
0.84	1.62	3520.51	5.21
0.95	1.61	3520.51	5.22
1.11	1.62	3520.51	5.21
1.28	0.39	3613.52	3.60
1.48	1.60	3651.11	11.08
1.60	1.64	3680.44	4.72

Pet			
pH	A	Frequency (1/cm)	dipole (Debyes)
0.84	1.83	3520.56	6.91
0.95	1.84	3520.56	6.92
1.11	1.83	3520.56	6.91
1.28	0.96	3625.44	5.44
1.48	1.49	3645.10	1.77
1.60	1.75	3669.67	6.23

Where A is the absorbance (without unit), ε the molar extinction coefficient (in $L.mol^{-1}.cm^{-1}$) and l the optical path (in cm) and C is the concentration of the solution (mol/lit) so, it has been calculated the values of ε in Table 2 for pigments of Cya, Del, Mal, Pel, Peo, Pet in different pH.

By plotting the chart of absorbance (A) versus concentration of H^+, it has been gained the high relation coefficients for Mal, Del, and Pel anthocyanins in water; see following first order of linear equations with the best relation coefficient for Mal pigment (Figure 2a,b) and compared to three other pigments of Cya, Peo, and Pet with low relation coefficients.

For colorless compounds, it is sometimes possible to manufacture colored complexes. This law is only valid for low concentrations and, in general, for absorbance of less than 1. However, this will depend on the solute studied and the quality of the spectrophotometer. In all cases, to ensure that the law is verified in the chosen field of study, it suffices to plot the absorbance as a function of the concentration. Beyond a certain concentration, linearity is no longer obtained beyond a certain concentration. It is, therefore, necessary to make dilutions to remain in the linear domain.

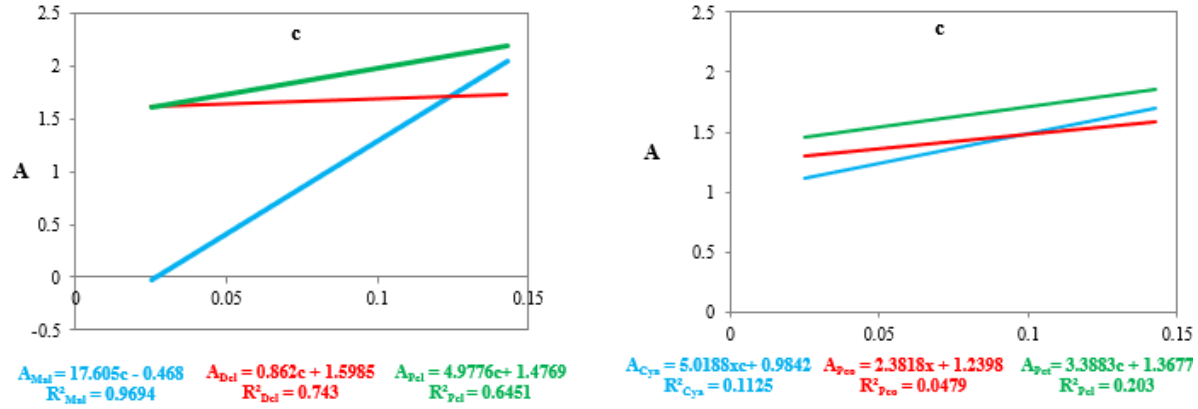

Figure2. Changes of absorbance **(A)** versus concentration of H^+ **(c)** for anthocyanin pigments of **(a)** Mal, Del, Pel with high relation coefficient and **(b)** Cya, Peo, Pet with low relation coefficient.

In the present project, the optimized models of anthocyanin pigments have been applied to estimate the absorbance of indicated molecules toward exhibiting the stabilization and range of color due to their electronic structures in vacuum and water media with different concentrations of H^+. So, the absorbance equation versus concentration has been accomplished the best value of relation coefficient for Mal, Del, Pel colored pigments in contrast to the relation coefficient for Cya, Peo, Pet colored pigments by fitting the values in table 2 (Figure 2a,b).

As it has been seen in Table 1, the physical properties of high Frequency and Dipole moment of Cya, Del, Mal, Pel, Peo, and Pet were calculated in different weak acidic media by infrared computational method (Figure 3a,b).

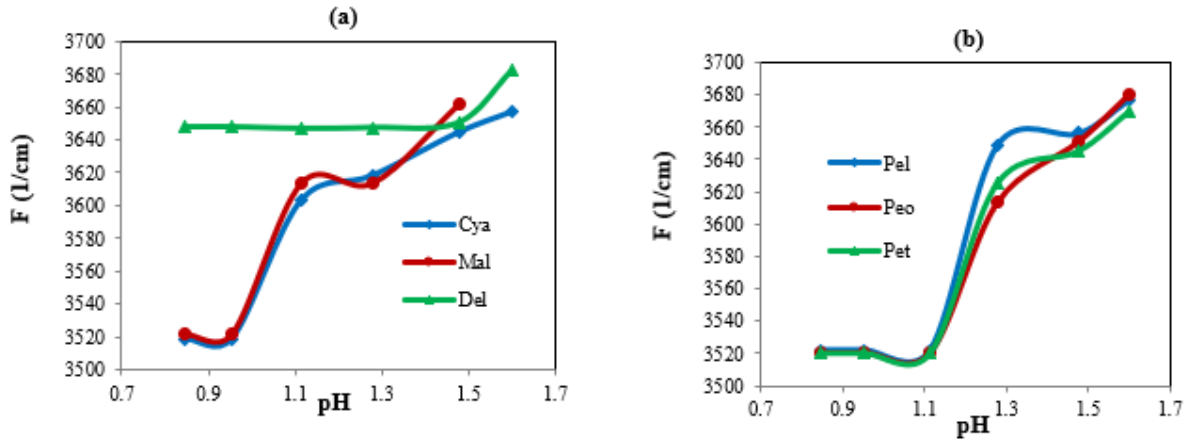

Figure 3. Changes of Frequency **(F)** versus pH for anthocyanin pigments of **(a)** Cya, Mal, Del, and **(b)** Pel, Peo, Pet.

Among the most common implicit solvation models, there is the PCM model. Since the solvent used is water at basic pH, it is recommended to use the PCM model.

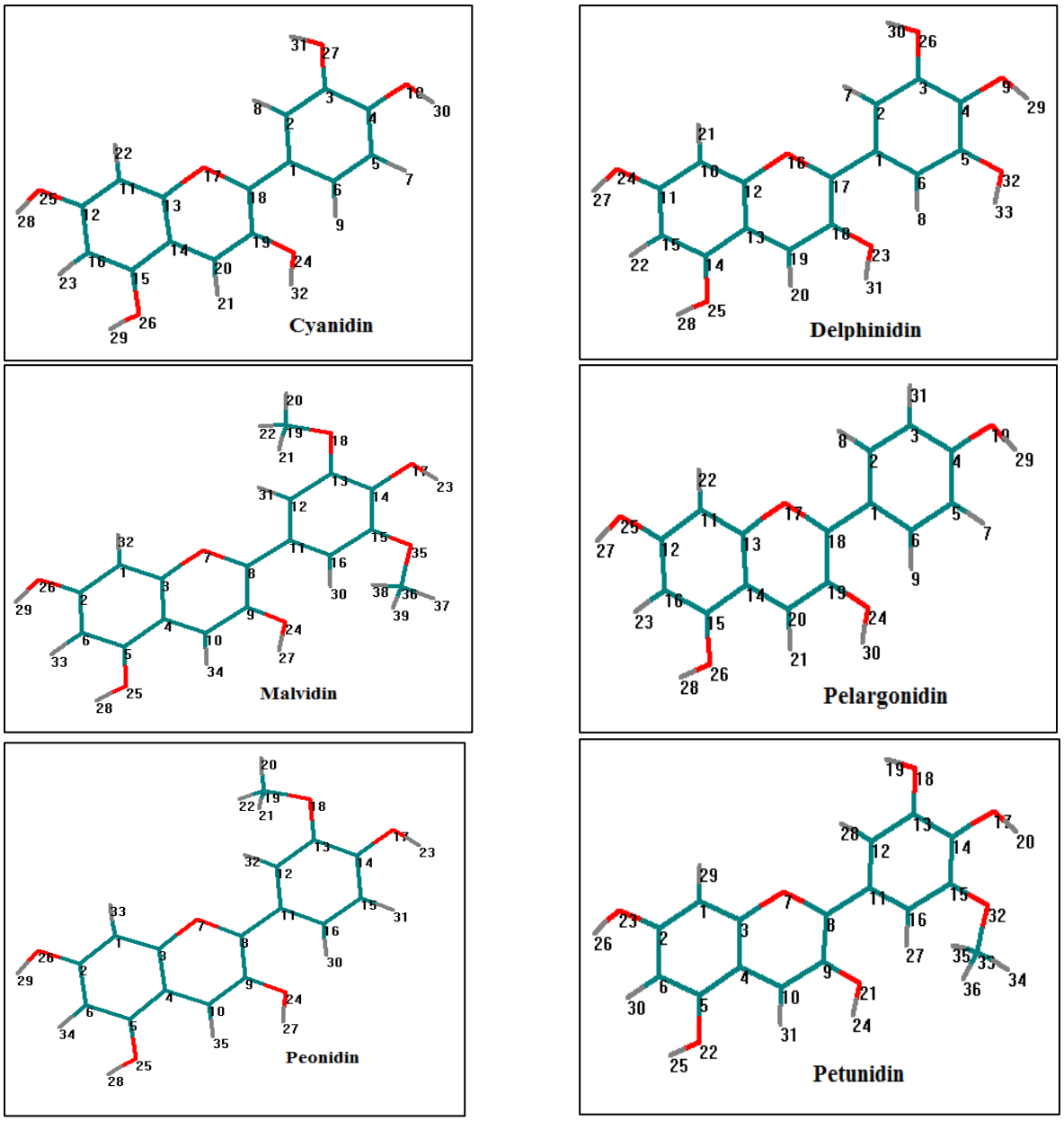

Figure 4. The 3D Isosuface schematics of calculated total spin density for different atoms in anthocyanins; Cyanidin (O_{17}), Delphinidin, Malvidin (O_7), Pelargonidin (O_{17}), Peonidin (O_7), and Petunidin (O_7).

However, the choice of one model has no significant impact on the free energies of the species studied nor on the stability of the structures. However, this model has many limitations; one of the most important is that they do not take into account the dynamic aspect of the effects between the solute and the solvent. Despite this, these solvation methods can be used in order to improve the energies and geometries of chemical species involved in reaction mechanisms.

Table 3. The atomic charge for Oxygen atoms in molecules of Cyanidin, Delphinidin, Malvidin, Pelargonidin, Peonidin, and Petunidin in different media of vacuum and water.

Atom	Cya (vacuum)	Cya (water)
O10	-0.23	-0.26
O17	-0.16	-0.17
O24	-0.26	-0.24
O25	-0.24	-0.24
O26	-0.25	-0.24
O27	-0.24	-0.25
	Del (vacuum)	**Del (water)**
O9	-0.23	-0.24
O16	-0.16	-0.16
O23	-0.26	-0.26
O24	-0.24	-0.23
O25	-0.25	-0.22
O26	-0.23	-0.24
O32	-0.27	-0.27
	Mal/(vacuum)	**Mal/(water)**
O7	-0.16	-0.15
O17	-0.23	-0.24
O18	-0.17	-0.17
O24	-0.26	-0.24
O25	-0.25	-0.24
O26	-0.24	-0.21
O35	-0.20	-0.19
	Pel/(vacuum)	**Pel/(water)**
O10	-0.25	-0.26
O17	-0.16	-0.16
O24	-0.26	-0.25
O25	-0.24	-0.24
O26	-0.25	-0.24
	Peo/(vacuum)	**Peo/(water)**
O7	-0.16	-0.17
O17	-0.23	-0.24
O18	-0.17	-0.24
O24	-0.26	-0.24
O25	-0.25	-0.23
O26	-0.24	-0.24
	Pet/(vacuum)	**Pet/(water)**
O7	-0.16	-0.16
O17	-0.23	-0.24
O18	-0.23	-0.24
O21	-0.26	-0.25
O22	-0.25	-0.22
O23	-0.24	-0.23
O32	-0.20	-0.20

The vibrational results accomplished of IR spectra have illustrated the normal mode of the active parts of anthocyanin pigments of Cya, Del, Mal, Pel, Peo, and Pet in weak acidic optimized media to approve the stability and color of these compounds. In addition, the

principal vibrational modes were considered based on the stability and color of different anthocyanin pigments (Table 2 and Figure 3a,b).

Besides, in this work, the atomic charge of oxygen in six electrophilic structures of anthocyanin pigments (Cya, Del, Mal, Pel, Peo, and Pet) has been extracted as the active parts of the molecules which are responsible for the electron charge transfer toward generating a range of various colored and water-soluble anthocyanins in water compared to vacuum medium (Figure 4 and Table 3).

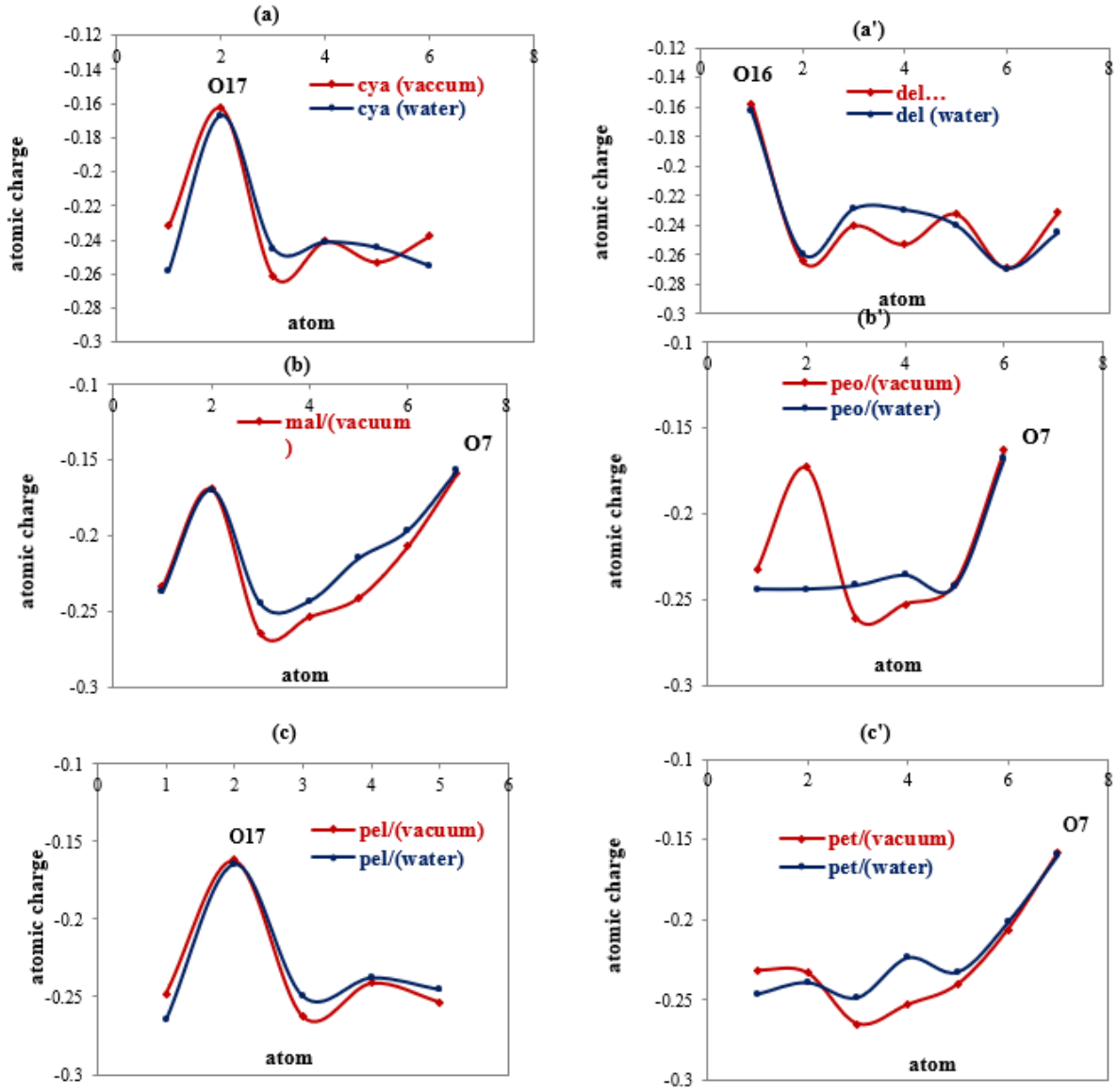

Figure 5. Comparison of atomic charge for oxygen atoms in molecules of **(a)** Cya **(b)** Mal **(c)** Pel and **(a')** Del **(b')** Peo **(c')** Pet in vacuum and water media.

So far, we have validated the choice of the functional, the base, and the model of solvation employees. The calculations were all carried out under normal temperature conditions at 300K. However, the conditions of microfluidic synthesis are more extreme. It is necessary to consider this when calculating because the Gibbs free energy of a system is influenced by temperature. Therefore, it is judicious to establish the profile of respective energies of the studied species as a function of temperature.

In Figure5(a-c, a'-c'), it has been plotted the fluctuation of atomic charge of oxygen atoms based on optimized molecules (Figure4) and data in table 3 of the electrophilic groups

of Cya, Del, Mal, Pel, Peo, and Pet in vacuum in comparison to water ,a polar medium, with high dielecrtic constant (≈80) which conduct us to explore the stability and color of these structures in the natural products of vegetables and fruits.

The perspective of Figure 5 suggests that the different data observed in Cya, Del, Mal, Pel, Peo, and Pet are fundamentally linked to the situation of active parts of oxygen atoms in these molecules which pass the electron charge in aromatic cyclic chains due to water polar molecules (Figure 6a,b).

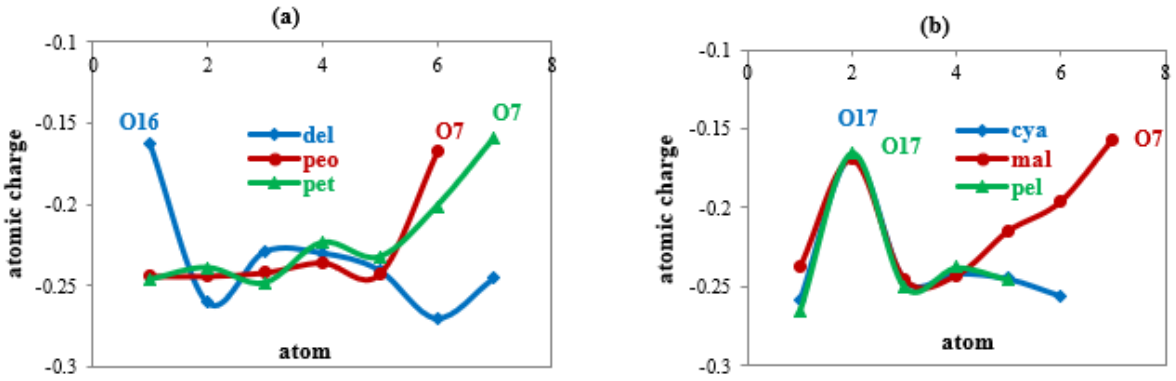

Figure 6. Fluctuation of the atomic electron charge for Oxygen atoms in anthocyanins of **(a)** Del, Peo, Pet, and **(b)** Cya, Mal, Pel in water at 300K.

4. Conclusions

The raw materials described above nevertheless have the potential to be used as a source of dyes. They have hues to cover the range of colors, from the bright red of black strawberry cherry to the dark red of red cabbage. In addition, recent advances in formulation open up good prospects for all fruits and vegetables with high concentrations of anthocyanins.

Modeling and simulation methods on pigments of Cya, Del, Mal, Pel, Peo, Pet describes the absorbance parameter in vacuum and water media and then unravel the stabilization energy and geometry which have been affected by the infrared theoretical method through the evaluation of the thermodynamic properties and the electronic structural of identified compounds.

The data have shown that such extrapolation schemes significantly overestimate the anthocyanin pigments by sharp parts of electrophilic molecules in weakly acidic media with different concentrations of H^+, which are the most active particles at the applied compounds in this project toward a large range of research due to building up the health-promoting.

Funding

This research received no external funding.

Acknowledgments

This research has no acknowledgment.

Conflicts of Interest

The authors declare no conflict of interest.

References

1. Ziemlewska, A.; Zagórska-Dziok, M.; Nizioł-Łukaszewska, Z. Assessment of cytotoxicity and antioxidant properties of berry leaves as by-products with potential application in cosmetic and pharmaceutical products. *Scientific Reports* **2021**, *11*, https://doi.org/10.1038/s41598-021-82207-2.
2. Silva, G.R.; Vaz, C.V.; Catalão, B.; Ferreira, S.; Cardoso, H.J.; Duarte, A.P.; Socorro, S. Sweet Cherry Extract Targets the Hallmarks of Cancer in Prostate Cells: Diminished Viability, Increased Apoptosis and Suppressed Glycolytic Metabolism. *Nutr. Cancer* **2020**, *72*, 917-931, https://doi.org/10.1080/01635581.2019.1661502.
3. Correia, P.; Oliveira, H.; Araújo, P.; Brás, N.F.; Pereira, A.R.; Moreira, J.; de Freitas, V.; Mateus, N.; Oliveira, J.; Fernandes, I. The Role of Anthocyanins, Deoxyanthocyanins and Pyranoanthocyanins on the Modulation of Tyrosinase Activity: An *In vitro* and *In silico* Approach. *International Journal of Molecular Sciences* **2021**, *22*, https://doi.org/10.3390/ijms22126192.
4. Kondo, T.; Hagihara, S.; Takaya, Y.; Yoshida, K. Polyacylated Anthocyanins in Bluish-Purple Petals of Chinese Bellflower, Platycodon grandiflorum. *International Journal of Molecular Sciences* **2021**, *22*, https://doi.org/10.3390/ijms22084044.
5. Fonseca, L.R.S.; Silva, G.R.; Luís, Â.; Cardoso, H.J.; Correia, S.; Vaz, C.V.; Duarte, A.P.; Socorro, S. Sweet Cherries as Anti-Cancer Agents: From Bioactive Compounds to Function. *Molecules* **2021**, *26*, https://doi.org/10.3390/molecules26102941.
6. Ohshima, K.; Morii, E. Metabolic Reprogramming of Cancer Cells during Tumor Progression and Metastasis. *Metabolites* **2021**, *11*, https://doi.org/10.3390/metabo11010028.
7. Wang, L.; Jiang, G.; Jing, N.; Liu, X.; Li, Q.; Liang, W.; Liu, Z. Bilberry anthocyanin extracts enhance anti-PD-L1 efficiency by modulating gut microbiota. *Food & Function* **2020**, *11*, 3180-3190, https://doi.org/10.1039/D0FO00255K.
8. Molina-Montes, E.; Salamanca-Fernández, E.; Garcia-Villanova, B.; Sánchez, M.J. The Impact of Plant-Based Dietary Patterns on Cancer-Related Outcomes: A Rapid Review and Meta-Analysis. *Nutrients* **2020**, *12*, https://doi.org/10.3390/nu12072010.
9. Sun, Y.; Zhang, Y.; Xu, W.; Zheng, X. Analysis of the anthocyanin degradation in blue honeysuckle berry under microwave assisted foam-mat drying. *Foods* **2020**, *9*, https://doi.org/10.3390/foods9040397.
10. Chialva, C.; Blein, T.; Crespi, M.; Lijavetzky, D. Insights into long non-coding RNA regulation of anthocyanin carrot root pigmentation. *Scientific Reports* **2021**, *11*, https://doi.org/10.1038/s41598-021-83514-4.
11. Kang, H.-J.; Ko, M.-J.; Chung, M.-S. Anthocyanin Structure and pH Dependent Extraction Characteristics from Blueberries (Vaccinium corymbosum) and Chokeberries (Aronia melanocarpa) in Subcritical Water State. *Foods* **2021**, *10*, https://doi.org/10.3390/foods10030527.
12. LaFountain, A.M.; Yuan, Y.-W. Repressors of anthocyanin biosynthesis. *New Phytologist* **2021**, *231*, 933-949, https://doi.org/10.1111/nph.17397.
13. Tahan, A.; Mollaamin, F.; Monajjemi, M. Thermochemistry and NBO analysis of peptide bond: Investigation of basis sets and binding energy. *Russian Journal of Physical Chemistry A* **2009**, *83*, 587-597, https://doi.org/10.1134/S003602440904013X.
14. Ghalandari, B.; Monajjemi, M.; Mollaamin, F. Theoretical Investigation of Carbon Nanotube Binding to DNA in View of Drug Delivery. *J.Comput.Theor.Nanosci* **2011**, *8*, 1212-1219, https://doi.org/10.1166/jctn.2011.1801.
15. Mollaamin, F.; Monajjemi, M.; Salemi, S.; Baei, M.T. A Dielectric Effect on Normal Mode Analysis and Symmetry of BNNT Nanotube. *FullerenesNanotubes and Carbon Nanostructure* **2011**, *19*, 182-196, https://doi.org/10.1080/15363831003782932.
16. Frisch, M.; Trucks, G.W.; Schlegel, H.B.; Scuseria, G.E.; Robb, M.A.; Cheeseman, J.R.; Scalmani, G.; Barone, V.; Mennucci, B.; Petersson, G. gaussian 09, Revision d. 01, Gaussian. *Inc., Wallingford CT* **2009**, *201*, https://gaussian.com/g09citation/.
17. Alvarez-Suarez, J.M.; Cuadrado, C.; Redondo, I.B.; Giampieri, F.; González-Paramás, A.M.; Santos-Buelga, C. Novel approaches in anthocyanin research-Plant fortification and bioavailability issues. *Trends Food Sci. Technol.* **2021**, *29*, https://doi.org/10.1016/j.tifs.2021.01.049.
18. Pina, F.; Alejo-Armijo,A.; Clemente, A.; Mendoza,J.; Seco,A.; Nuno Basílio,N.; and ,A.J. Evolution of Flavylium-Based Color Systems in Plants: What Physical Chemistry Can Tell Us. *Int. J. Mol. Sci.* **2021**, *22*, https://doi.org/10.3390/ijms22083833.

19. Mollaamin, F.; Ilkhani, A.; Sakhaei, N.; Bonsakhteh, B.; Faridchehr, A.; Tohidi, S.; Monajjemi, M. Thermodynamic and Solvent Effect on Dynamic Structures of Nano Bilayer-Cell Membrane: Hydrogen Bonding Study. *Journal of Computational and Theoretical Nanoscience* **2015**, *12*, 3148-3154, https://doi.org/10.1166/jctn.2015.4092.
20. Monajjemi, M.; Afsharnezhad, S.; Jaafari, M.R.; Mirdamadi, S.; Mollaamin, F.; Monajemi, H. Investigation of energy and NMR isotropic shift on the internal rotation Barrier of Θ4 dihedral angle of the DLPC: A GIAO study. *Chemistry* **2008**, *17*, 55-69, https://www.researchgate.net/publication/257140202_Investigation_of_energy_and_NMR_isotropic_shift_on_the_internal_rotation_Barrier_of_TH4_dihedral_angle_of_the_DLPC_A_GIAO_study.
21. Asraoui, F.; Kounnoun, A.; Cadi, H.E.; Cacciola, F.; Majdoub, Y.O.; Alibrando, F.; Mandolfino, F.; Dugo, P.; Mondello, L.; Louajri, A. Phytochemical Investigation and Antioxidant Activity of Globularia alypum L. *Molecules* **2021**, *26*, https://doi.org/10.3390/molecules26030759.
22. Monajjemi, M.; Mollaamin, F.; Gholami, M.R.; Yoosbashizadeh, H.; Sadrnezhad, S.K.; Passdar, H. Quantum Chemical Parameters of Some Organic Corrosion Inhibitors, Pyridine, 2-Picoline 4-Picoline and 2, 4-Lutidine, Adsorption at Aluminum Surface in Hydrocholoric and Nitric Acids and Comparison Between Two Acidic Media. *Main Group Met. Chem.* **2003**, *26*, 349-362, https://doi.org/10.1515/MGMC.2003.26.6.349.
23. Faienza, M.F.; Corbo, F.; Carocci, A.; Catalano, A.; Clodoveo, M.L.; Grano, M.; Wang, D.Q.H.; D'Amato, G.; Muraglia, M.; Franchini, C.; Brunetti, G.; Portincasa, P. Novel insights in health-promoting properties of sweet cherries. *Journal of Functional Foods* **2020**, *69*, https://doi.org/10.1016/j.jff.2020.103945.
24. Tiss, M.; Souiy, Z.; Achour, L.; Hamden, K. Anti-obesity, anti-hyperglycaemic, anti-antipyretic and analgesic activities of Globularia alypum extracts. *Arch. Physiol. Biochem*. **2020**, 1-8, https://doi.org/10.1080/13813455.2020.1773865.
25. Monajjemi, M.; Mahdavian, L.; Mollaamin, F.; Khaleghian, M. Interaction of Na, Mg, Al, Si with carbon nanotube (CNT): NMR and IR study. *Russian Journal of Inorganic Chemistry* **2009**, *54*, 1465-1473, https://doi.org/10.1134/S0036023609090216.
26. Sarasia, E.M.; Afsharnezhad, S.; Honarparvar, B.; Mollaamin, F.; Monajjemi, M. Theoretical study of solvent effect on NMR shielding tensors of luciferin derivatives. *PCL* **2011**, *49*, 561-571, https://doi.org/10.1080/00319101003698992.
27. Arena, K.; Cacciola, F.; Rigano, F.; Dugo, P.; Mondello, L. Evaluation of matrix effect in one-dimensional and comprehensive two-dimensional liquid chromatography for the determination of the phenolic fraction in extra virgin olive oils. *J. Sep. Sci.* **2020**, *43*, 1781-1789, https://doi.org/10.1002/jssc.202000169.
28. El Cadi, H.; El Cadi, A.; Kounnoun, A.; Oulad El Majdoub, Y.; Palma Lovillo, M.; Brigui, J.; Dugo, P.; Mondello, L.; Cacciola, F. Wild strawberry (Arbutus unedo): Phytochemical screening and antioxidant properties of fruits collected in northern Morocco. *Arabian Journal of Chemistry* **2020**, *13*, 6299-6311, https://doi.org/10.1016/j.arabjc.2020.05.022.
29. Liu, X.; Wang, L.; Jing, N.; Jiang, G.; Liu, Z. Biostimulating Gut Microbiome with Bilberry Anthocyanin Combo to Enhance Anti-PD-L1 Efficiency against Murine Colon Cancer. *Microorganisms* **2020**, *8*, https://doi.org/10.3390/microorganisms8020175.
30. Ahles, S.; Joris, P.J.; Plat, J. Effects of Berry Anthocyanins on Cognitive Performance, Vascular Function and Cardiometabolic Risk Markers: A Systematic Review of Randomized Placebo-Controlled Intervention Studies in Humans. *International Journal of Molecular Sciences* **2021**, *22*, https://doi.org/10.3390/ijms22126482.
31. Onali, T.; Kivimäki, A.; Mauramo, M.; Salo, T.; Korpela, R. Anticancer Effects of Lingonberry and Bilberry on Digestive Tract Cancers. *Antioxidants* **2021**, *10*, 850, https://doi.org/10.3390/antiox10060850.
32. Li, L.; Luo,C.; and Zheng,X. Purification of Anthocyanins Derived from Black Kidney Bean (Phaseolus vulgaris L.) by a Simulated Moving Bed. *Journal of Chemistry* **2021**, *2021*, https://doi.org/10.1155/2021/5580756.
33. Houghton, A.; Appelhagen, I.; Martin, C. Natural Blues: Structure Meets Function in Anthocyanins. *Plants* **2021**, *10*, 726, https://doi.org/10.3390/plants10040726.
34. Yoshida, K.; Ito, D.; Miki, N.; Kondo, T. Single-cell analysis clarifies mosaic color development in purple hydrangea sepal. *New Phytologist* **2021**, *229*, 3549-3557, https://doi.org/10.1111/nph.17099.
35. Mollaamin, F.; Monajjemi, M. Harmonic Linear Combination and Normal Mode Analysis of Semiconductor Nanotubes Vibrations, *J. Comput. Theor. Nanosci*. **2015**, *12*, 1030-1039, https://doi.org/10.1166/jctn.2015.3846.

36. Gai, Z.; Wang, Y.; Ding, Y.; Qian, W.; Qiu, C.; Xie, H.; Sun, L.; Jiang, Z.; Ma, Q.; Wang, L.; Ding, Z. Exogenous abscisic acid induces the lipid and flavonoid metabolism of tea plants under drought stress. *Scientific Reports* **2020**, *10*, https://doi.org/10.1038/s41598-020-69080-1.
37. Mendoza, J.; Oliveira, J.; Araújo, P.; Basílio, N.; Teixeira, N.; Brás, N.F.; Pina, F.; Yoshida, K.; de Freitas, V. The peculiarity of malvidin 3-O-(6-O-p-coumaroyl) glucoside aggregation. Intra and intermolecular interactions. *Dyes and Pigments* **2020**, *180*, 108382**,** https://doi.org/10.1016/j.dyepig.2020.108382.
38. Monajjemi, M.; Baie, M.T.; Mollaamin, F. Interaction between threonine and cadmium cation in [Cd(Thr) n]2+ (n = 1–3) complexes: density functional calculations, *Russian Chemical Bulletin* **2010**, *59*, 886-889, https://doi.org/10.1007/s11172-010-0181-5.
39. Monajjemi, M.; Khaleghian, M.; Tadayonpour, N.; Mollaamin, F. The Effect Of Different Solvents And Temperatures On Stability Of Single-Walled Carbon Nanotube: A Qm/Md Study. *International Journal of Nanoscience* **2010**, *09*, 517-529, https://doi.org/10.1142/S0219581X10007071.
40. Vilkickyte, G.; Raudone, L.; Petrikaite, V. Phenolic Fractions from Vaccinium vitis-idaea L. and Their Antioxidant and Anticancer Activities Assessment. *Antioxidants* **2020**, *9*, https://doi.org/10.3390/antiox9121261.
41. Khaleghian, M.; Zahmatkesh, M.; Mollaamin, F.; Monajjemi, M. Investigation of Solvent Effects on Armchair Single-Walled Carbon Nanotubes: A QM/MD Study. *Fullerenes Nanotubes and Carbon Nanostructures* **2011**, *19*, 251-261, https://doi.org/10.1080/15363831003721757.
42. Kirkwood, J.G. The Dielectric Polarization of Polar Liquids. *J. Chem. Phys.* **1939**, *7*, 911, https://doi.org/10.1063/1.1750343.
43. Onsager, L. Electric Moments of Molecules in Liquids. *Journal of the American Chemical Society* **1936**, *58*, 1486-1493, https://doi.org/10.1021/ja01299a050.
44. Wong, M.W.; Frisch, M.J.; Wiberg, K.B. Solvent effects. 1. The mediation of electrostatic effects by solvents. *Journal of the American Chemical Society* **1991**, *113*, 4776-4782, https://doi.org/10.1021/ja00013a010.
45. Bakhshi, K.; Mollaamin, F.; Monajjemi, M. Exchange and Correlation Effect of Hydrogen Chemisorption on Nano V(100) Surface: A DFT Study by Generalized Gradient Approximation (GGA). *Journal of Computational and Theoretical Nanoscience* **2011**, *8*, 763-768, https://doi.org/10.1166/jctn.2011.1750.
46. Monajjemi, M.; Noei, M.; Mollaamin, F. Design of fMet-tRNA and Calculation of its Bonding Properties by Quantum Mechanics. *Nucleosides, Nucleotides & Nucleic Acids* **2010**, *29*, 676-683, https://doi.org/10.1080/15257771003781642.
47. Zadeh, M.A.A.; Lari, H.; Kharghanian, L.; Balali, E.; Khadivi, R.; Yahyaei, H.; Mollaamin, F.; Monajjemi, M. Density Functional Theory Study and Anti-Cancer Properties of Shyshaq Plant: In View Point of Nano Biotechnology. *Journal of Computational and Theoretical Nanoscience* **2015**, *12*, 4358-4367, https://doi.org/10.1166/jctn.2015.4366.
48. Li, X.; Hong, Y.; Jackson, A. *et al.* Dynamic regulation of small RNAs in anthocyanin accumulation during blueberry fruit maturation. *Sci Rep* **2021**, *11*, 15080, https://doi.org/10.1038/s41598-021-93141-8.
49. Mauramo, M.; Onali, T.; Wahbi, W.; Vasara, J.; Lampinen, A.; Mauramo, E.; Kivimäki, A.; Martens, S.; Häggman, H.; Sutinen, M.; Salo, T. Bilberry (Vaccinium myrtillus L.) Powder Has Anticarcinogenic Effects on Oral Carcinoma *In vitro* and *In vivo*. *Antioxidants* **2021**, *10*, 1319, https://doi.org/10.3390/antiox10081319.
50. Yan,H.; Pei,X.; Zhang,H.; Li,X.; Zhang,X.; *et al*. MYB-Mediated Regulation of Anthocyanin Biosynthesis. *Int. J. Mol. Sci.* **2021**, *22*, 3103, https://doi.org/10.3390/ijms22063103.
51. Mauramo, M.; Onali, T.; Wahbi, W.; Vasara, J.; Lampinen, A. et.al. Bilberry (Vaccinium myrtillus L.) Powder Has Anticarcinogenic Effects on Oral Carcinoma *In vitro* and *In vivo*. *Antioxidants* **2021**, *10*, 1319, https://doi.org/10.3390/antiox10081319.
52. Dong, N.; Lin, H. Contribution of phenylpropanoid metabolism to plant development and plant-environment interactions. *J. Integr. Plant Biol.* **2021**, *63*, 180-209, https://doi.org/10.1111/jipb.13054.